MMP9 cleavage of the β4 integrin ectodomain leads to recurrent epithelial erosions in mice

Sonali Pal-Ghosh[1], Tomas Blanco[2], Gauri Tadvalkar[1], Ahdeah Pajoohesh-Ganji[1], Arpitha Parthasarathy[1], James D. Zieske[2] and Mary Ann Stepp[1,3,*]

[1]The George Washington University Medical Center, Department of Anatomy and Regenerative Biology, Washington, DC 20037, USA
[2]The Schepens Eye Research Institute, Harvard Medical School, Boston, MA 02114, USA
[3]The George Washington University Medical Center, Department of Ophthalmology, Washington, DC 20037, USA
*Author for correspondence (mastepp@gwu.edu)

Accepted 1 April 2011
Journal of Cell Science 124, 2666-2675

doi:10.1242/jcs.085480

Summary

Integrin α6β4 is an integral membrane protein within hemidesmosomes and it mediates adhesion of epithelial cells to their underlying basement membrane. During wound healing, disassembly of hemidesmosomes must occur for sheet movement-mediated cell migration. The mechanisms of disassembly and reassembly of hemidesmosomes are not fully understood. The current study was initiated to understand the underlying cause of recurrent corneal erosions in the mouse. Here, we show that in vivo: (1) MMP9 levels are elevated and β4 integrin is partially cleaved in epithelial cell extracts derived from debridement wounded corneas; (2) the β4 ectodomain is missing from sites where erosions develop; and (3) β4 cleavage can be reduced by inhibiting MMP activity. Although β4, α3 and β1 integrins were all cleaved by several MMPs, only MMP9 was elevated in cell extracts derived from corneas with erosions. Coimmunoprecipitation studies showed that β4 integrin associates with MMP9, and protein clustering during immunoprecipitation induced proteolytic cleavage of the β4 integrin extracellular domain, generating a 100 kDa β4 integrin cytoplasmic domain fragment. Confocal imaging with three-dimensional reconstruction showed that MMP9 localizes at erosion sites in vivo where the ectodomain of β4 integrin is reduced or absent. MMP activation experiments using cultured corneal and epidermal keratinocytes showed reduced levels of α6β4 and β1 integrins within 20 minutes of phorbol ester treatment. This report is the first to show that β4 integrin associates with MMP9 and that its ectodomain is a target for cleavage by MMP9 in vivo under pathological conditions.

Key words: Integrins, MMPs, Keratinocytes, Wound healing

Introduction

Healing of the corneal epithelium after injury is rapid and takes place by sheet movement. Hemidesmosomes mediate attachment of the epithelial basal cells to their basement membrane and disassemble upon injury to facilitate the sliding of the sheet across the exposed basement membrane zone (BMZ) (Gipson, 1992; Gipson et al., 1993). Adherens junctions, desmosomes and tight junctions are all still present in the migrating corneal epithelial sheet but are less abundant towards the leading edge (Suzuki et al., 2000; Suzuki et al., 2003; Hutcheon et al., 2007). After migration is complete, cell–cell adhesions reform, first at the sealed wound margins, and later at the wound periphery along with the hemidesmosomes. Hemidesmosomes consist of two integral membrane components: the α6β4 integrin heterodimer and collagen XVII/BPA180 (Stepp et al., 1990; Nishizawa et al., 1993; Borradori and Sonnenberg, 1996). Genetically engineered mice lacking β4 integrin have no hemidesmosomes and lose their epithelium at birth (van der Neut et al., 1996; Dowling et al., 1996). Patients with mutations that reduce the expression or function of α6β4 integrin have subtypes of epidermolysis bullosa (EB) and develop skin blisters because of the reduced structural integrity of their hemidesmosomes (Uitto and Richards, 2004; de Pereda et al., 2009). Patients with mutations in collagen XVII develop a subtype of EB or a related disease called bullous pemphigoid (BP) (Zillikens and Giudice, 1999; Schumann et al., 2000).

Our lab has developed a mouse model to reproducibly induce recurrent epithelial erosions that spontaneously arise within 2 weeks after a single corneal debridement wound (Pal-Ghosh et al., 2004). These erosions occur but with different frequencies in both C57BL6 and BALB/c mice strains (Pal-Ghosh et al., 2008). The current study was initiated to determine the mechanism behind the development of erosions. Studies of patients with recurrent corneal erosions have shown elevated levels of various MMP family members (Garrana et al., 1999; Ramamurthi et al., 2006). Elevated levels of MMPs are also seen in dry eye disease (Chotikavanich et al., 2009). We hypothesized that at sites of erosion, activated MMPs could cleave basement membrane proteins, leading to internalization and degradation of α6β4 integrin, thereby destabilizing adhesion of epithelial cells to the underlying BMZ. Instead, we report that α6β4 integrin itself was targeted for cleavage by activated MMP9 during erosion formation.

Results

Rapid corneal epithelial sheet migration after debridement causes recurrent erosions in the periphery of the cornea

The speed of corneal re-epithelialization after wounding is remarkable. At 18 hours after a small wound involving removal of ~35% of corneal epithelium, 90% of the wound area is covered. Large wounds involving removal of 85–90% of the corneal epithelium are over 60% closed within 18 hours (Fig. 1). This rapid migration rate requires an equally rapid rate of disassembly of the hemidesmosomes at the basal surface of the unwounded corneal epithelium. However, rapid re-epithelialization can result in detachment of the epithelial sheet from the underlying surface during or soon after re-epithelialization. This delays wound closure and increases the risk of infection. Unless hemidesmosomes

reassemble after migration is complete, resolution of healing will be delayed. Using a mouse cornea debridement model, recurrent epithelial erosions can be induced in the cornea after a single debridement wound (Pal-Ghosh et al., 2004).

If the failure to reassemble hemidesmosomes were the primary cause of the recurrent erosions, we would expect that erosions would form at the center of the cornea where wounds are made and hemidesmosome disassembly is maximal because leading edges merge at the center of the cornea. Also, large wounds, which involve disassembly of hemidesmosomes over a larger surface area, would be expected to show more erosion. Our lab has shown that there are fewer erosions after large wounds, and this difference is significant (Pal-Ghosh et al., 2004). To address the question of where the erosions form, we examined 14 eyes after small wounds and 39 eyes after large wounds 6 weeks after wounding.

Data on the location of the erosions are presented in Fig. 1. To test the hypothesis that erosions form centrally, we used the Chi-square test. The following assumptions were made: expected values for centrally located erosions were 11 of 12, and 29 of 30, for small and large wounds, respectively; 2 of the 14 cornea with small wounds and 9 of the 39 corneas with large wounds were closed at 4 weeks and had no erosions. Of corneas with erosions, 1 of 12 (8%) and 8 of 30 (27%) were in the central region after small and large wounds, respectively, which is significantly fewer than expected ($P<0.001$) by the Chi-square test. We then tested the assumption that the erosions in the periphery are distributed randomly around the corneal circumference, we found significantly ($P<0.001$) more erosions in the nasal periphery (66% and 52% for small and large wounds, respectively) compared with the other regions. These results indicate that: (1) erosions are not caused exclusively by delayed reassembly of hemidesmosomes after wound healing, and (2) the anatomy of the mouse eye has a significant role in the development of erosions.

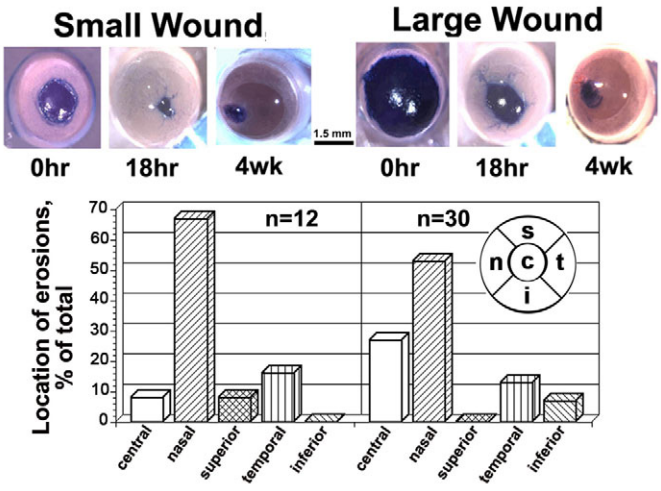

Fig. 1. Epithelial sheets move rapidly to close debridement wounds, but over time, recurrent erosions develop. Open wounds detected by Richardson stain at various times after wounding are shown in the top panel. Scale bar: 1.5 mm. The anatomical locations of the erosions that develop are shown graphically below as the percentage of the erosions that develop centrally or at the nasal, superior, temporal or inferior quadrants. Using Chi-squared statistics, after both small and large wounds, there are significantly more erosions in the periphery compared with the center of the cornea. In the periphery, there are more erosions in the nasal quadrant compared with all other quadrants combined ($P<0.001$).

Removal of the BMZ during injury increases β4 integrin production at the wound site and prevents erosions

In a TEM study performed to look at the structure of the BMZ after debridement, we showed that the lamina densa remains on the anterior stroma after wounding, but is progressively lost, first at the center, and later at the periphery (Sta Iglesia and Stepp, 2000). Wounds that remain open for more than 24 hours showed a complete loss of the lamina densa at sites where the stroma was exposed. Basal cells that initiate migration at the wound periphery move over a BMZ with an intact lamina densa, whereas cells at the center of the cornea migrate over a BMZ with no lamina densa.

These observations, coupled with data showing more erosions at the corneal periphery, suggest that residual lamina densa has a role in the formation of erosions. We tested this hypothesis by creating superficial keratectomy wounds. Unlike debridement wounds, superficial keratectomy wounds involve removal of the corneal epithelial cells along with their BMZ and a portion of the anterior stroma. As shown in images taken 6 weeks after wounding, there were no erosions seen by slit lamp or by fluorescein staining in any of the mouse corneas subjected to keratectomy injury, although a scar could be seen in the stroma at the periphery of the cornea (Fig. 2A).

Analysis of β4 integrin localization by confocal microscopy using an ectodomain directed antibody and 3D image reconstruction revealed an abrupt transition between the site where the keratectomy wound was made and the unwounded area peripheral to it. Within the keratectomy site, elevated levels of β4 integrin were observed (Fig. 2B). There were more epithelial cell layers within the keratectomy wound zone compared with adjacent sites. More β4 integrin was expressed per basal cell and in more cell layers within keratectomy sites compared with levels in adjacent regions (Fig. 2C). Corneal epithelial cells were extracted 4 weeks after injury by limbal to limbal debridement and used for immunoblot analyses of β4 integrin expression. Immunoblots obtained using a C-terminal tail directed β4 integrin antibody confirmed that production of the ~200 kDa full-length β4 integrin protein was twice as high in keratectomy wounded corneas compared with unwounded corneas (Fig. 2D).

Healing of debridement wounds is accompanied by degradation and focal loss of β4 integrin ectodomain at erosion sites

Next, we examined debridement wounds as a function of time after wounding for differences in expression and localization of β4 integrin by immunoblots and confocal imaging (Fig. 3A–D). As expected from our previous studies, β4 integrin expression increased within corneal epithelial cells during the active phase of re-epithelialization and remained above control levels for 1 week after both sizes of wounds. Full-length β4 integrin is ~200 kDa with a ~100 kDa ectodomain and a ~100 kDa cytoplasmic domain. Using an antibody against the C-terminal cytoplasmic tail of β4 integrin, we observed a 200 kDa band corresponding to full-length β4 integrin and a series of lower molecular mass bands. These results show that the β4 integrin N-terminus is subjected to proteolytic cleavage, reducing the size of the protein from 200 kDa to 160 kDa. We also saw 100 and 50 kDa fragments. When these fragments were quantified and presented graphically

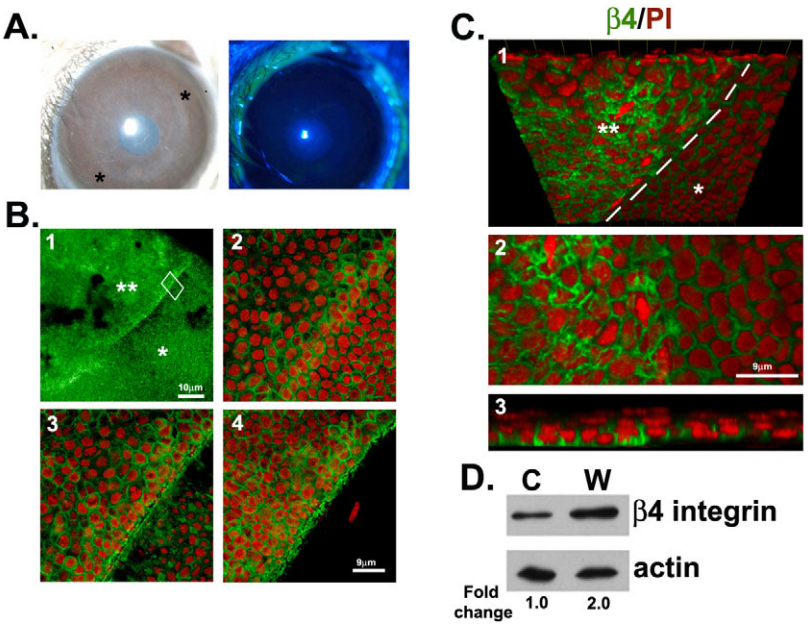

Fig. 2. Basement membrane removal prevents erosions and enhances β4 integrin localization and expression within the injury site. (**A**) Keratectomy wounded eyes 4 weeks after wounding. Eyes were evaluated for open wounds with both slit lamp and 2% fluorescein eye drops. The two asterisks in the slit lamp image indicate the margins of the wound seen as a scar after 4 weeks. (**B**) β4 staining of 4-week cornea in green at 10× magnification (1). The double white asterisks indicate the keratectomy-wounded area and single asterisk, the unwounded area. (2) A 63× image of boxed area in 1. Images 2–4 are taken from apical to basal at 2–3 μm intervals. (**C**) 3-D reconstruction of a keratectomy wounded area at 63× (1). The image has been tilted at a 45° angle so the β4 staining can be seen basally. The dotted lines indicate the boundary between wounded and unwounded area. Image 2 is a magnified view of 1, showing the increased expression of β4 and image 3 is a cross-sectional view of 1 highlighting the increased number of cell layers at the keratectomy site. (**D**) Immunoblots of corneal epithelium from control and keratectomy corneas show that 4-week keratectomy-wounded corneal epithelia express more β4 integrin than control epithelia.

(supplementary material Fig. S1), there is evidence of increased cleavage of β4 integrin during active re-epithelialization.

To examine the localization of β4 integrin after debridement wounding, we used confocal microscopy and 3D image reconstruction with an antibody against the β4 integrin ectodomain rather than the cytoplasmic domain. Results shown in Fig. 3C indicate a loss of the β4 integrin ectodomain at and around erosion sites. Higher resolution imaging was performed (Fig. 3D) and showed β4 integrin surrounding the basal cells of the corneal epithelium of control corneas, at the leading edge during active re-epithelialization at 18 hours, and adjacent to the erosion site 4 weeks after large wounds. Results show that erosions are accompanied by focal loss of the β4 integrin ectodomain within clusters of epithelial cells.

Upregulation of MMP9 protein and mRNA and focal expression of MMP9 protein are seen in corneas with recurrent erosions

To determine whether the levels of MMP proteins are elevated during erosion formation, we performed zymography using extracts from control and 4-week wounded corneas. Data shown in Fig. 4A indicate that there is an upregulation of MMPs with molecular mass over 100 kDa in all four corneas with erosions. MMP2 (72 kDa) and MMP3 (54 kDa) were expressed in control and wounded corneas. In two of four corneas assessed, MMP3 was elevated compared with the control. MMP9 is often referred to as the 92 kDa gelatinase, which reflects its size in human cells; in the mouse, it is larger and is over 100 kDa in corneal tissues (Mohan et al., 2002). To determine whether *Mmp9* mRNA was also elevated in corneas with erosions, mRNA was isolated from control and wounded corneas for QPCR (Fig. 4B). The level of *Mmp9* mRNA was below detectable limits in all control samples (n=6) evaluated. However, 4 weeks after large wounds, three of four samples tested expressed *Mmp9* mRNA. These data implicate elevated levels of MMP9 in the etiology of recurrent erosions after debridement wounds.

Based on the zymogram and QPCR results and on studies showing an important role for MMP9 in maintenance of the ocular surface epithelial barrier (Pflugfelder et al., 2005), we proceeded to assess the expression of MMP9 protein as a function of time after injury by immunoblotting (Fig. 4C). We found that MMP9 protein levels were elevated at 18 hours and 2 days after small and large wounds compared with controls, and remained elevated at 1 and 4 weeks after wounding.

Next, we assessed the localization of MMP9 on the ocular surface using whole-mount confocal microscopy. MMP9-positive epithelial cells were seen at and around erosion sites 4 weeks after injury (Fig. 4D). 3D image reconstruction showed no detectable MMP9 in control corneal epithelium. MMP9 is expressed in a few suprabasal cells adjacent to the leading edge 18 hours after debridement wounding and localized within cells at and adjacent to the erosion site 4 weeks after wounding (Fig. 4E).

MMPs and TACE cleave β4 integrin in addition to α3 and β1 integrins

To determine whether MMP2, MMP3 and/or MMP9 cleave β4 integrin, we extracted proteins from mouse epidermal keratinocytes without protease inhibitors and assayed for the susceptibility of β4, α3 and β1 integrins to cleavage by three activated MMPs (MMP2, MMP3, MMP9) or by TACE (TNF-α converting enzyme/ADAM17). TACE is included in these experiments because it is an MMP family member that has been implicated in the corneal epithelial erosions that develop after exposure of eyes to mustard gas (Mol et al., 2009). After 60 minutes, extracts with no MMPs added showed a time-dependent reduction in the amount of full-length β4 integrin as a result of the action of endogenous proteases (Fig. 5A). MMP2, MMP3 and MMP9 all cleaved β4 integrin and eliminated the ~200 kDa band within 5 minutes. TACE also cleaved β4 integrin, but cleavage was slower. Prolonged exposure of immunoblots similar to those shown in Fig. 5A showed that cleavage by both MMP2 and MMP9 generated a 100 kDa fragment (see supplementary material Fig. S2).

To determine whether other integrins are susceptible to cleavage by MMPs and TACE, we assessed the degradation of α3 and β1 integrins using C-terminal-directed antibodies. α3 integrin showed

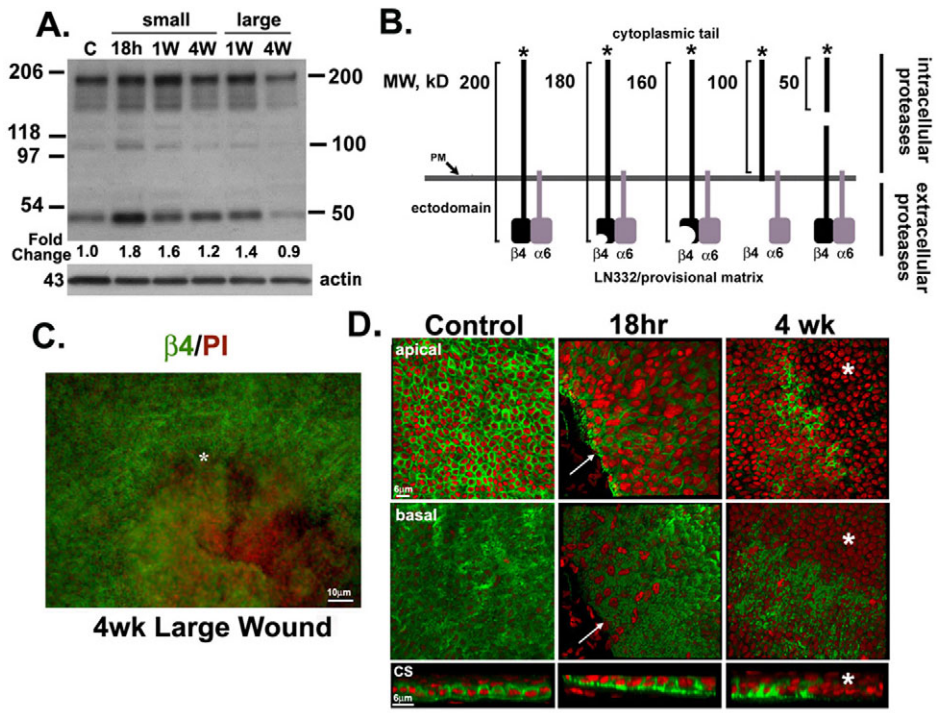

Fig. 3. The appearance of β4 integrin degradation products during healing of debridement wounds is accompanied by the loss of the β4 integrin ectodomain adjacent to erosions. (**A**) Immunoblots of corneal epithelia harvested at different time points probed with β4 integrin and actin showing the fold change in β4 integrin expression over time compared with control. Blots show formation of proteolytic cleavage products derived from β4 integrin during wound healing of small and large wounds. Quantification of these bands are shown in supplementary material Fig. S1. (**B**) Schematic representation of the types of cleavage products expected from cleavage of β4 integrin into different size fragments. Fragments over 100 kDa, are derived from the action of extracellular proteases whereas fragment less than 100 kDa are derived from intracellular proteases. (**C**) 10× image showing the loss of β4 at erosion site (*) 4 weeks after wounding with β4 in green and PI in red. (**D**) 3D reconstruction of 63× images of control, 18 hour and 4 week tissues stained with β4 and PI showing apical, basal and cross sectional (CS) views of the corneal epithelium. The white arrows indicate the leading edge at 18 hours and the asterisks indicate the erosion site with loss of β4 integrin.

differential susceptibility for cleavage by MMPs and TACE; it was sensitive to MMP3 and was completely degraded in 30 minutes, but was resistant to cleavage by MMP9 and TACE. MMP2 rapidly degraded a fraction of the α3 integrin. β1 integrin was resistant to cleavage by MMP2 and was sensitive to MMP3, MMP9 and TACE. MMP3 almost completely degraded β1 integrin by 60 minutes in a time-dependent manner. There was a rapid reduction in the level of β1 integrin after MMP9 and TACE were added to the samples, but no further loss of protein over the 60 minute time period. The partial sensitivity to degradation of α3 and β1 suggests that there are MMP-sensitive and -resistant pools of these integrins in cells.

To confirm that endogenous MMPs present within corneal epithelial cells are capable of cleaving integrins, extracts from unwounded and wounded corneal epithelia were incubated without protease inhibitors, with a protease inhibitor cocktail (+PI), or with GM6001, which is a broad-spectrum MMP inhibitor. Because epithelial extracts from animals 18 hours after wounding have 1.8-fold more β4 integrin (Fig. 3A) and 4.7-fold more MMP9 (Fig. 4C) compared with control epithelial extracts, these experiments allow us to determine whether elevated MMP9 levels alter the sensitivity of β4 integrin to degradation.

When no inhibitors were added to unwounded extracts, the amount of full-length β4 integrin decreased, and 80% was degraded by 5 hours. Adding a PI cocktail partially delayed β4 degradation and 60% was degraded by 5 hours (Fig. 5B). When the MMP inhibitor GM6001 was added to control extracts, a doublet appeared over time. When both β4 bands were summed and the percentage degradation calculated, in the presence of GM6001, only 10% of β4 integrin was degraded in extracts from control cornea.

There was more full-length β4 integrin in extracts obtained from corneas 18 hours after wounding. When no inhibitors were added to wounded extracts, β4 integrin was degraded more rapidly over time and intact β4 was below detectable levels by 5 hours. Adding the PI cocktail delayed β4 degradation during the first hour, after which β4 integrin was rapidly degraded and was also below detectable levels by 5 hours. By contrast, when the MMP inhibitor was added, more full-length β4 integrin was observed at time 0 and the rate of degradation over the time course was slowed. Compared with PI-treated samples in which 100% of the β4 integrin degraded by 5 hours, GM6001-treated samples had degraded by 75% at this time point. These data show that β4 integrin is sensitive to proteolytic cleavage by endogenous proteases and MMPs. When MMP levels are low, in unwounded extracts, cleavage can be almost entirely blocked by MMP inhibitors, but when MMP-levels are elevated after wounding, it was not possible to block β4 integrin cleavage over time.

MMP activation in vitro induces a rapid but modest reduction in total and surface integrin

Numerous studies have been performed using the phorbol ester TPA (tissue plasminogen activator) to activate MMPs and induce shedding of various surface proteins, including syndecan-1; these

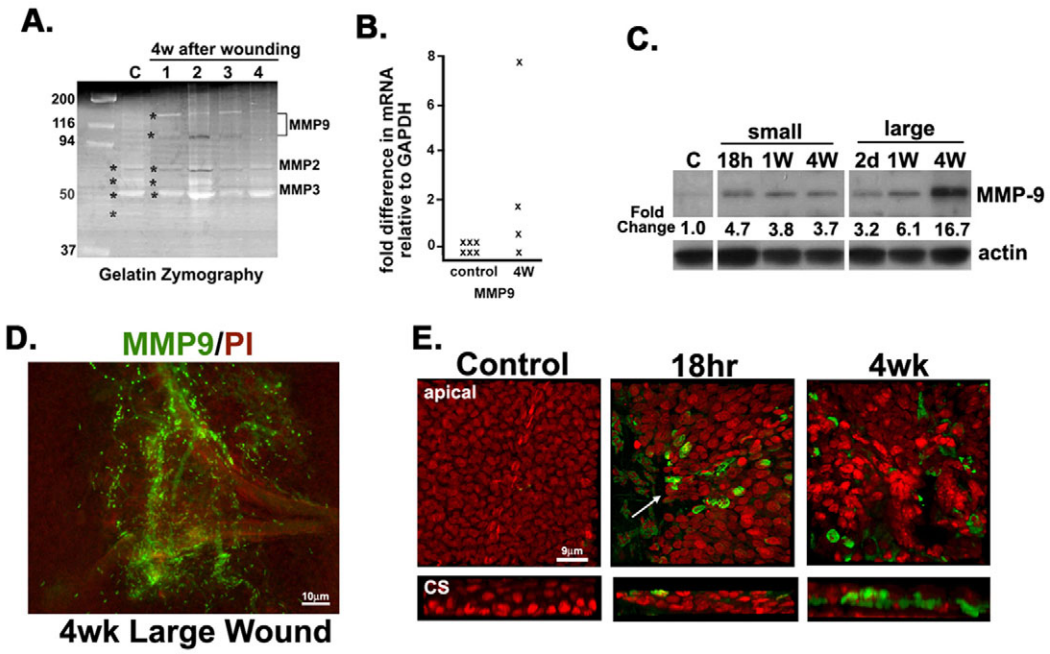

Fig. 4. MMP9 is upregulated at the mRNA and protein levels in corneas with erosions. (**A**) Gelatin zymography of four epithelial tissue extracts taken 4 weeks after wounding compared with a control extract shows increased MMP activity for proteins with molecular mass consistent with that of MMP9. Asterisks indicate the mobility of each of the major bands detected. (**B**) QPCR performed on mRNA isolated from corneal epithelia shows below detectable mRNA levels for MMP9 before wounding in all control samples evaluated (n=6 animals) and increased levels in three of four samples after wounding. Each '×' represents RNA from two corneas and data are expressed relative to *Gapdh* mRNA levels. (**C**) Immunoblots of corneal epithelial samples at different time points probed with MMP9 and actin showing the fold change in MMP9 expression compared with control. (**D**) 10× magnification image of the erosion site indicating increased MMP9 in green. (**E**) 3D reconstruction of 63× images at control, 18 hours and 4 weeks after wounding shown en face and in cross section (CS). The arrow in the 18 hour image indicates the MMP9-positive cells at the leading edge. The area adjacent to the erosion site at 4 weeks (4W) shows a loss of tissue organization and increased levels of MMP9 expression.

cleavage events are mediated by TACE (Pruessmeyer et al., 2010) and/or MMP7 (Chen et al., 2009) and inhibited by MMP inhibitors (Ludwig et al., 2005). To determine whether α6β4 integrin is shed from keratinocyte surfaces after TPA treatment, we incubated human corneal epithelial cells in medium with 0.02% DMSO or TPA in 0.02% DMSO. Although antibodies directed against α6 and β4 integrin ectodomains work well for staining tissues and cells, they often do not function for immunoblotting. Because shedding of the integrin ectodomains leaves the cytoplasmic tails of these molecules behind on cell surfaces, cell culture medium cannot be used to evaluate shed α6β4 integrin. We extracted cells at 20, 60 and 180 minutes after treatment with 100 mM TPA and performed immunoblots. TPA treatment reduced the levels of all three integrins assessed (β4, α6 and α3) at 20 minutes; α3 integrin levels had partially recovered by 180 minutes (Fig. 5C). To look directly at surface integrin expression, we performed flow cytometry studies using mouse epidermal keratinocytes treated with two different concentrations of TPA (100 mM and 200 mM) for 20 minutes. Similar results were obtained at both TPA concentrations (Fig. 5D). Surface levels of β1 integrin were significantly reduced; however, levels of β4 integrin, although also lower, did not achieve statistical significance.

MMP9 associates with and induces cleavage of the β4 integrin ectodomain

MMP9 was chronically elevated in debridement-wounded corneas when erosions formed (Fig. 4) and β4 integrin was subject to MMP-mediated cleavage (Fig. 5B), but the experiments shown do not distinguish which MMPs are responsible for β4 cleavage. MMP9 could degrade β4 integrin directly or it could degrade integrin ligands and cause degradation of β4 integrin indirectly. If β4 integrin is a direct MMP9 target, the two proteins should associate with one another.

Coimmunoprecipitation experiments were thus performed using epithelial extracts from unwounded and wounded corneas 4 weeks after injury. We immunoprecipitated with β4 integrin or MMP9 antibodies and immunoblotted with antibodies against the β4 integrin cytoplasmic domain or MMP9 (Fig. 6). When β4 integrin was subjected to immunoprecipitation, the full-length 200 kDa protein was observed, but the majority of β4 integrin immunoprecipitated from both control and wounded samples at 4 weeks was present as a 100 kDa C-terminal fragment, consistent with cleavage of the entire ectodomain; β4 integrin immunoprecipitates from wounded corneas showed the presence of MMP9. When MMP9 was immunoprecipitated, no full-length β4 integrin was seen; however, the 100 kDa C-terminal fragment was observed in both control and wounded samples. As shown schematically in Fig. 6, the association between the β4 integrin ectodomain and MMP9 during immunoprecipitation induced degradation of β4 integrin, leaving a 100 kDa fragment containing the C-terminal intracellular domain, which resisted further MMP-mediated degradation.

The experiments presented above show that β4 integrin and MMP9 associate, and this association induces MMP9 cleavage of the β4 integrin ectodomain. If MMP9 is capable of associating with and/or cleaving β4 integrin in vivo at erosion sites, there

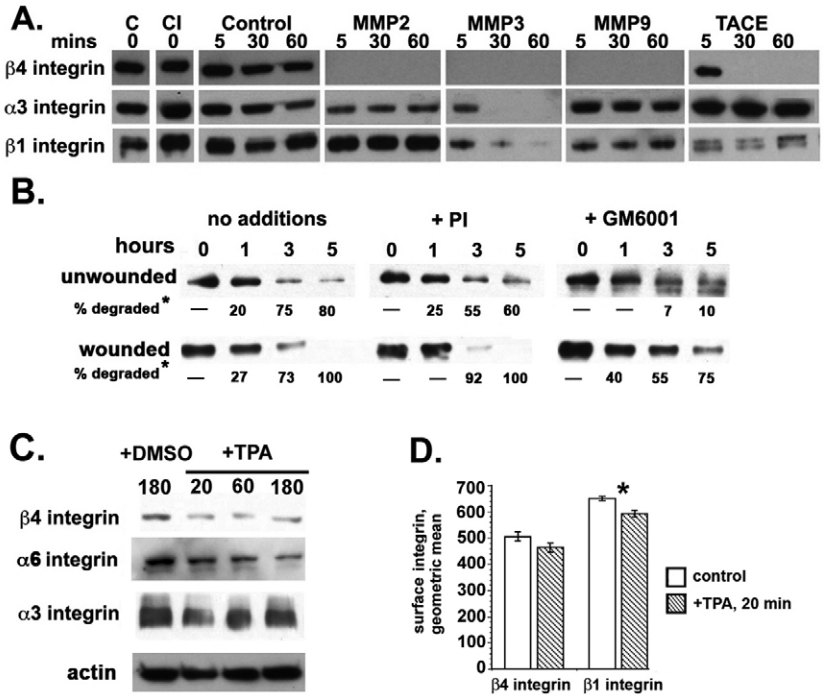

Fig. 5. MMPs and TACE cleave β4 integrin, which can be partially inhibited by GM6001 and protease inhibitors, and TPA induces a rapid loss of α6 and β4, but not α3 integrin. (**A**) The study of MMP-specific degradation of integrins by MMPs and TACE at 5, 30 and 60 minutes. A longer exposure of the β4 integrin data is provided in supplementary material Fig. S2. (**B**) Extracts from unwounded and 18-hour-wounded corneas were used to compare the rate of cleavage of β4 integrin with and without addition of a protease inhibitor cocktail or the MMP inhibitor GM6001. The asterisk indicates that data were quantified and the percentage degradation calculated relative to the amount of β4 integrin present at time 0. For unwounded GM6001-treated extracts, both β4 bands were summed for the calculations. Data show that in unwounded corneas, GM6001 can block most of the β4 integrin degradation, but can only delay degradation in wounded corneas. (**C**) MMP activation was induced by TPA and integrin degradation studied in human corneal epithelial cells. Cells were treated with 0.02% DMSO for 180 minutes as controls and with 0.02% DMSO plus TPA for 20, 60 and 180 minutes. Data show a rapid decrease in all three integrins studied at 20 minutes; by 180 minutes, α3 integrin expression partially recovered, whereas expression of β4 and α6 integrin remained lower than DMSO-treated control cells. (**D**) MMP activation was induced by TPA and β4 and β1 integrin ectodomain shedding studied in primary mouse epidermal keratinocytes 20 minutes after treatment using flow cytometry. Data indicate a significant reduction in β1 integrin on cell surfaces after MMP activation (*P<0.05); the reduction in β4 surface expression was not quite statistically significant.

should be less β4 integrin ectodomain detected on cells where MMP9 is localized. 3D confocal imaging was performed on whole mounts of corneas with erosions to study the colocalization of MMP9 and the β4 integrin ectodomain. There was an absence of the β4 integrin ectodomain within cells expressing MMP9 (Fig. 7), but we did observe focal but infrequent colocalization of the β4 integrin ectodomain and MMP9. Our in vitro studies show that MMP9 can associate with and cleave β4 integrin, and the in vivo studies confirm that β4 ectodomain cleavage occurs and contributes to the focal development of recurrent erosions in the cornea.

Discussion

The data presented here, obtained using in vivo and in vitro approaches, show that: (1) MMP9 expression is elevated in the mouse corneal epithelium at erosion sites; (2) the ectodomain of β4 integrin is lost focally within the corneal epithelial sheet and adjacent to erosion sites where MMP9 is also expressed; (3) MMP9 associates with and degrades β4 integrin; (4) β4 integrin cleavage is inhibited by an MMP-inhibitor; and (5) α6β4 and β1 integrin cleavage are induced rapidly in cultured human corneal epithelial cells and mouse epidermal keratinocytes by MMP activation. Our studies also show that MMPs and TACE target other integrins in addition to β4 integrin.

The fact that β4 integrin is easily degraded was appreciated soon after it was identified (Kennel et al., 1989). β4 integrin is degraded by calpain (Giancotti et al., 1992; Potts et al., 1994) and by caspase-3 and caspase-7 (Werner et al., 2007). The intracellular cleavage of β4 integrin by calpain and caspases generates a β4 integrin cytoplasmic domain truncation that cannot mediate cytoskeletal assembly and hemidesmosome formation, induces rapid proteasomal degradation of β4 integrin, and sensitizes cells to apoptosis (Werner et al., 2007). Because β4 integrin is roughly 200 kDa with approximately 100 kDa inside and 100 kDa outside the cell, caspase- and/or calpain-mediated degradation cannot account for the generation of cleavage products with molecular masses of 100 kDa or larger assessed using an antibody against the C-terminal-tail of β4 integrin. Only proteases that act on the ectodomain of β4 integrin generate fragments 100 kDa or larger in size. Although a report describing the ability of matrilysin/MMP7 to cleave β4 integrin derived from human prostate cell line extracts has appeared in the literature (von Bredow et al., 1997), additional investigations of this topic have not been reported. Interestingly, there has been a report that MMP9 can induce the shedding of the β2 family integrins on immune cells (Vaisar et al., 2009). Not only does this shedding inhibit adhesion of leukocytes to inflamed

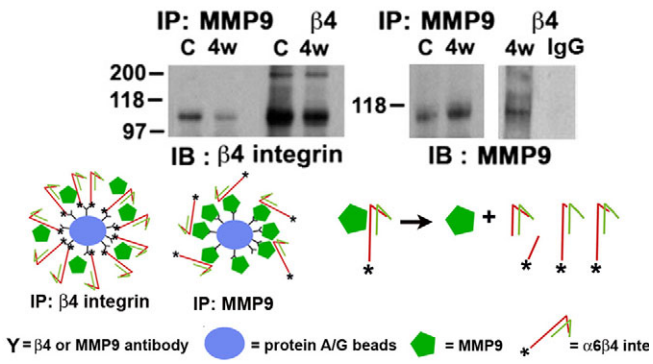

Fig. 6. MMP9 coimmunoprecipitates with and cleaves full-length β4 integrin. Control (C) and wounded (4w) tissues were immunoprecipitated with antibodies against the β4 integrin cytoplasmic domain and MMP9. Blots probed with the β4 cytoplasmic domain antibody reveal that MMP9 and full-length β4 integrin associate with one another and this association induces β4 integrin cleavage. Blots probed with antibody against MMP9 reveal that MMP9 is present in β4 integrin immunoprecipitates. Beads incubated with control IgG are also shown. The diagram in the lower panel schematically shows protein A/G beads coated with either β4 integrin or MMP9 antibodies and incubated with corneal epithelial cell extracts containing α6β4 and MMP9. MMP9 associates with the β4 integrin extracellular domain and cleaves it. The expected degradation products are shown on the left. The symbols used to represent protein A/G, MMP9 and β4 integrin are also shown.

tissues, but also the shed molecules appear to act as dominant-negative inhibitors of CD11 or CD18 function on leukocytes (Gjelstrup et al., 2010).

Our data are the first to show that β4 integrin associates with and is cleaved by MMP9. Other studies have used coimmunoprecipitation to show that MMP9 associates with β1 integrin (Radjabi et al., 2008) and CD11 or CD18 (Vaisar et al., 2009), that MMP2 associates with α5β1 and αv integrins (Menon et al., 2006; Morozevich et al., 2009; Chetty et al., 2010; Choi et al., 2010), and that MT1-MMP associates with both αv- and β1-containing integrins on endothelial cells (Gálvez et al., 2002). The study by Menon and colleagues (Menon et al., 2006) shows that the association between α5β1 integrin and MMP2 induces apoptosis of rat myocytes after stimulation by β-adrenergic receptor and the study by Radjabi and colleagues (Radjabi et al., 2008) shows thrombin induced tumor cell invasion by enhancing the association of MMP9 and β1 integrin. The majority of these studies used immunoprecipitation with an integrin antibody followed by immunoblotting for the MMP so it is not possible to determine whether immunoprecipiation induced integrin cleavage.

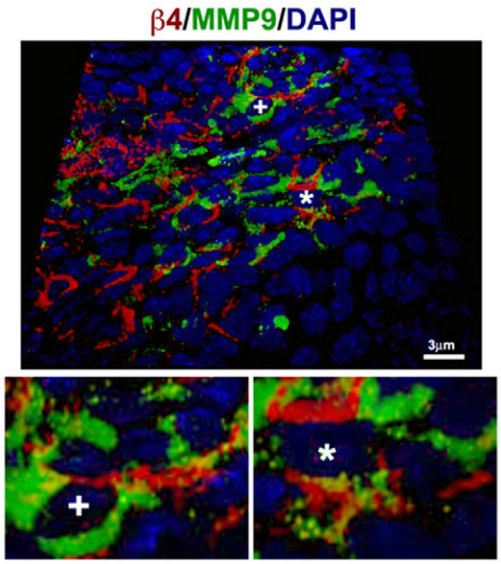

Fig. 7. MMP9 induces β4 integrin ectodomain cleavage in vivo at sites of erosions. 3D image at 63× magnification of a 4-week cornea with erosion. The areas labeled with '+' and '*' have been digitally magnified 3× to reveal times focal sites of colocalization of MMP9 and β4 integrin ectodomain.

One experimental method used to assess MMP-activated shedding of cell surface molecules is to treat cells with TPA (Ludwig et al., 2005). TPA has been shown to induce the activation of several different MMP family members including MT1-MMP, TACE/ADAM17, ADAM10 and MMP7 (Endo et al., 2003; Ludwig et al., 2005; Chen et al., 2009; Pruessmeyer et al., 2010); TPA-induced ectodomain shedding of numerous cell surface proteins can be blocked by specific MMP inhibitors (Ludwig et al., 2005). MMPs are often upregulated in cultured cells in vitro, during cancer development and dissemination, and in numerous pathological conditions in vivo. We show here that TPA induced a rapid shedding of a portion of the α6β4 and α3β1 integrins from the surface of corneal epithelial and epidermal keratinocytes in vitro. Although an exhaustive survey of MMP family members to determine which are capable of cleaving α6β4 and α3β1 integrins is beyond the scope of this study, the association of MMP9 and β4 integrin in corneal epithelial extracts suggests that MMP9-mediated cleavage of α6β4 integrin occurs in vivo and in migrating cells in vitro and in vivo.

Debridement-wounded mouse corneas obtained several weeks after wounding showed focal MMP9 localization and β4 integrin ectodomain loss at erosion sites. The elevated MMP9 protein could derive from immune cells trapped within the epithelial sheet at the erosion site. Regardless of the source, the presence of the elevated levels of MMP9 on the ocular surface for prolonged times leads to pathology. Erosions in the mouse cornea are prevented by removing the basement membrane at the time of injury. This may be due to better epithelial–stromal interaction, elimination of factors released by injured epithelial cells, the presence of BMZ fragments underlying the epithelial sheet, or to a combination of all three processes.

The fact that some of the MMP9 expressed in control epithelial tissues associates with β4 integrin and that they coimmunoprecipitate, indicates that the interaction of these two proteins does not always result in cleavage of the integrin. Our studies of MMP9 expression in control and wounded corneas did not show evidence for conversion of proMMP9 to active MMP in response to wounding, perhaps because differences in the mobility of murine pro- and active-MMP9 are too subtle to be seen in the gel system we used. MMP9 is an extracellular protease that binds to the extracellular domain of β4 integrin and if MMP9 were activated within a MMP9–β4-integrin complex, it would degrade the integrin. MMP9 immunoprecipitates would then not contain β4 integrin because the β4 integrin cytoplasmic domain does not bind to MMP9. The fact that the size of the major β4 integrin fragment detected in these coimmunoprecipitates is 100 kDa, indicates that cleavage was induced during sample processing and the cytoplasmic fragment of β4 integrin was trapped on the Sepharose beads during precipitation.

If inactive proMMP9–β4-integrin forms a complex in vivo under homeostatic conditions, what might the function of this complex be? Studies of the role of MMP9–β2-integrin associations indicate that proMMP9 associates with β2 integrin intracellularly and is expressed at the cell surface upon activation of leukocytes (Stefanidakis et al., 2004). Thus, the interaction of MMP9 with integrins might help to localize MMP9 at the cell surface. Other studies, again on immune cells, suggest that complexes of proMMP9 with integrin function as docking sites for CD44v (Redondo-Muñoz et al., 2008). Additional studies in epithelial tissues are needed to determine the exact role of MMP9 in the regulation of β4 integrin activity and function in health and disease.

Materials and Methods

Manual corneal debridement

All experiments described were conducted in voluntary compliance with the ARVO Statement for the Use of Animals in Ophthalmic and Vision Research. All procedures for debridement and keratectomy wounds were approved by the George Washington University Animal Care and Use Committee. BALB/c mice were obtained from NCI-Frederick; C57Bl6j mice were obtained from Jackson Labs (Bar Harbor, ME). For debridement wounding, 8- to 10-week-old mice (22–25 g) were anesthetized with 250 µl of a 1:10 dilution of a 1:1 mixture of ketamine (100 mg/ml; Aveco, Fort Dodge, IA) and xylazine (20 mg/ml; Miles, Shawnee Mission, KS). Once animals were anesthetized, a topical anesthetic (proparacaine ophthalmic solution) was applied to their ocular surfaces until the blink sensation was lost, and their corneas were scraped with a dull scalpel to remove the corneal epithelium as described previously (Pal-Ghosh et al., 2008). Corneas were allowed to heal in vivo for 18 hours, 1 week and 4 weeks for small and 2 days, 1 week and 4 weeks for large wounds. For keratectomy, 1.5 mm circular wounds were created in the central cornea as described previously (Hutcheon et al., 2005). An epithelial-stromal button was removed with forceps. The healing process was monitored under a slit lamp and the corneas were photographed before and after 2% fluorescein staining. The animals were allowed to heal for 4–6 weeks. Tissue extracts were derived from ten mouse corneas for each time point and each wound size and the data presented represent typical data from each study. Every in vivo experiment was conducted at least twice. To reduce the numbers of animals needed, only when discrepancies in experimental results were observed, were the in vivo studies repeated a third time.

After sacrifice, the corneal epithelium was either scraped and frozen in liquid nitrogen for RNA or protein biochemistry, or fixed for whole mounts as described previously (Pajoohesh-Ganji et al., 2004). A minimum of three eyes was used for each time point. For assessment of ocular surface integrity and erosion location, after sacrifice, the corneas of the BALB/c mice were sutured and stained with Richardson stain (1% methylene blue prepared in 1% borax mixed 1:1 with a 1% solution of azure II, filtered and stored at 4°C) to reveal exposed basement membrane and corneas were photographed. For assessment of the ocular surface in C57Bl6j mice after keratectomy wounds, mice were sacrificed at 6 weeks and slit lamp images captured before and after corneas were stained with 2% fluorescein. For the whole mount and biochemical studies of keratectomy wounds, mice were sacrificed at 4 weeks.

Whole mount and confocal microscopy

The tissues stored in 100% methanol were dissected to remove the lens, iris, and retina and four incisions were made equal distances apart to aid in flattening the corneas. Corneas were then processed for whole mounts as described previously (Pajoohesh-Ganji et al., 2004). The primary antibodies used for these studies are listed in Table 1. Secondary antibodies of the appropriate class were obtained from either Invitrogen or Molecular Probes conjugated with Alexa Fluor 488 or Alexa Fluor 594 (Molecular Probes, Invitrogen, Carlsbad, CA) or conjugated with Dylight 694 (Jackson ImmunoResearch Laboratories, West Grove, PA). Routine protocols included corneas stained with secondary antibodies alone. Corneas were stained with DAPI or propidium iodide before flat mounting to reveal nuclei. To achieve the best flattening, the corneas were placed epithelial side-up, mounting medium was added, followed by coverslips.

Confocal microscopy was performed at the Center for Microscopy and Image Analysis (CMIA) at the George Washington University Medical Center. A confocal laser-scanning microscope (model MRC 1024; Bio-Rad, Hercules, CA) equipped with a krypton-argon laser and an inverted microscope (model IX-70; Olympus) was used to image the localization of Alexa Fluor 488 (488 nm laser line excitation; 522/35 emission filter), Alexa Fluor 594 (568 nm excitation; 605/32 emission filter), and Dylight 694. Optical sections (z=0.5 mm) of confocal epifluorescence images were acquired sequentially with a 63× objective lens (NA 0.63) with image acquisition software (LaserSharp ver. 3.2; Bio-Rad). 63× images for keratectomy were acquired using the Ziess 710 using similar settings as the Bio-Rad confocal microscope. Typically, six to eight optical sections were merged and viewed en face. 3D images were obtained and rotated using Volocity software (Version 5.0; Perkin Elmer)

Table 1. Antibodies used for these studies

Antigen	Source	Catalog no. / Name	Application*
β1 integrin	Sta Iglesia et al., 2000	Rab27	IB
β1 integrin	Biolegend	HMβ1	FC
β4 integrin	Sta Iglesia et al., 2000	B4-7	IB, IF, IBAIP
β4 integrin	BD Pharmingen	553745	IF
β4 integrin	Biolegend	346-11A	FC
β6 integrin	Cell Signaling	3750	IB
β3 integrin	Sta Iglesia et al., 2000	A110	IB, IF
MMP9	Abcam	38898	IB, IF, IBAIP

*FC, flow cytometry; IB, Immunoblot; IP, Immunoprecipitation; IBAIP, Immunoblot after immunoprecipitation

Immunoblots and zymography

Immunoblot studies used corneal epithelium removed by debridement after specific time points. Epithelial tissues were extracted with 100 µl of Buffer A (0.1 M Tris-HCl, pH 8.5, 0.15 M NaCl, 0.5 mM $MgCl_2$ and 0.5% NP-40) with or without various additives to inhibit the activity of generic proteases or MMPs. For samples extracted in Buffer A plus the PI cocktail, to 2 ml Buffer A, 25 µl Pefabloc SC Plus (Roche), 286 µl 7× complete mini protease inhibitor (Roche Complete Mini) and 20 µl HALT phosphatase inhibitor cocktail (Pierce/ThermoFisher) were added. For samples incubated with MMP inhibitors, to 10 ml Buffer A, 4 µl of a 25 mM stock solution of Galardin/GM6001 (Sigma) was added. Protein assays were performed and equal amounts of total protein were loaded onto 4–20% Tris-glycine gels (Invitrogen) and electrophoresis was performed at 140 V. The proteins were transferred to PVDF membrane (Millipore) at 400 mA for 1.5 hours, and the blots blocked in 5% milk in TBS (10×) (Bio-Rad) with 0.1% Tween 20 (TBST) overnight at 4°C. Primary and secondary antibodies were added for 1 hour each at room temperature (RT), with washes in between. Blots were subjected to chemiluminescence using Pierce SuperSignalWestDura (Pierce), and chemiluminescence was detected using x-ray film. When appropriate, data were quantified using NIH ImageJ software. Each immunoblot or immunoprecipitation study used the epithelial tissues obtained from ten corneas for each time point.

For zymography, the tissues were extracted as mentioned above and equal amounts of protein were resolved using ReadyGel Precast Zymography Gels (Bio-Rad), bands were developed as described by the manufacturer and gels were photographed. Each lane shown in the gels used for zymography used the corneal epithelial tissues extracted from one mouse.

QPCR

Quantitative PCR was performed as described (Stepp et al., 2010). RNA was isolated from debrided corneal epithelia with TRIZOL (Invitrogen) following the manufacturer's protocol. For cDNA synthesis, 2 µg of total RNA was reverse transcribed using SuperScript III Reverse Transcriptase (Invitrogen). PCR amplifications were performed in a volume of 20 µl. For real-time PCR analysis, the expression level of MMP9 was determined using a Bio-Rad MYiQ iCycler and Gene Expression Macro (version 1.1). cDNA (diluted 1:200 in the final reaction) was measured from triplicate samples using iQ SYBR Green Supermix (Bio-Rad). The primer sequences for MMP9 and GAPDH were obtained from Qiagen. Relative standard curves were generated from log input versus the cycle threshold (C_t) and relative levels of cDNAs determined using the comparative C_t method with the cycle threshold difference corrected for GAPDH. Data are presented as fold change in gene expression normalized to GAPDH as described by Onat and colleagues (Onat et al., 2008). All experiments were performed in triplicate and used the epithelial tissues derived from ten corneas for each time point evaluated.

Keratinocyte cell culture

Primary mouse keratinocytes were derived from neonatal Balb/c mouse pups and were cultured as described previously (Stepp et al., 2007) and used after 3 days of culture in low-calcium medium. The human corneal and limbal epithelial (HCLE) cell line was a kind gift from Ilene Gipson (Schepen's Eye Research Institute, Harvard Medical School, Boston, MA). HCLE cells were grown in keratinocyte growth medium (Gibco) and were used at 70% confluence.

MMP degradation study

Epidermal keratinocytes were cultured for 3 days in low-calcium medium as described (Stepp et al., 2007). Purified recombinant mouse MMP2, MMP3 or MMP9 (all R&D Systems) were used after a 1 hour activation step with 4-aminophenylmercuric acetate (APMA) (Sigma) as described by the manufacturer. 2 µg activated purified MMP2, MMP3, MMP9 or TACE (R&D Systems) were used for each experiment. Cells were extracted in Buffer A without protease inhibitors and divided into five different aliquots and 2 µg of activated MMP2, MMP3, MMP9, TACE or buffer alone was added to each sample. Equal volumes of extract were removed 5, 30 and 60 minutes after incubation at 37°C and placed in 2× sample buffer to stop enzymatic

activity. Replicate samples were extracted in Buffer A plus PI cocktail. Samples were run onto gels and processed for immunoblotting. Experiments were repeated three times and the data shown represent typical experimental results.

Inhibition of β4 degradation using protease and MMP inhibitors

Unwounded or wounded mouse corneal epithelial tissues were harvested after 18 hours from ten mouse corneas by debridement. The epithelial cells were extracted in 100 µl Buffer A without any inhibitors. 15 µl of the extract was removed and 2× Laemmli sample buffer was added to serve as a control. The remaining extract was divided into three equal volumes and added to tubes containing an equal volume of Buffer A, Buffer A with 2× concentration of PI cocktail, or Buffer A plus a 2× concentration of GM6001. At 1, 3 and 5 hour time points, 15 µl was removed from each tube and added to 2× Laemmli sample buffer. All the samples were boiled for 5 minutes followed by gel electrophoresis and transfer. Each experiment required the use of epithelia from ten control and ten wounded corneas; experiments were repeated twice. The data presented show typical experimental results.

TPA-induced shedding

Human corneal epithelial cells were grown and treated with DMSO (ThermoFisher, #191418) only or DMSO plus TPA (Calbiochem, #524400) at a concentration of 100 mM. The final DMSO concentration in the media was maintained at 0.02%. After 20, 60 or 180 minutes, cells were extracted in Buffer A plus PI cocktail and equal amounts of total protein run onto SDS gels and processed for immunoblotting. Control cells had been incubated in DMSO alone for either 20 or 180 minutes. Experiments were repeated twice and the data shown represent typical results. Flow cytometry was performed using primary Balb/c mouse epidermal keratinocytes cultured as described previously (Stepp et al., 2007) treated with either 0.02% DMSO alone for controls, or with 100 mM or 200 mM TPA in 0.02% DMSO for 20 minutes. Experiments were repeated twice at each of the two concentrations of TPA and results were similar for all four experiments. The antibodies used to assess surface β1 and β4 integrins are indicated in supplementary material Table S1.

Immunoprecipitation followed by immunoblotting

Samples were extracted in either RIPA buffer (10× RIPA Lysis Buffer, Millipore) or with Buffer A [50 mM Tris-HCl, pH 8.0, 0.15 mM NaCl, 0.5 mM $CaC1_2$, 0.5% (v/v) Nonidet P-40]; a PI cocktail was added and extracts were pre-cleared with 30 µl of washed and packed Dynabeads (Invitrogen) for 15 minutes at room temperature. 3 µl of the appropriate primary antibody was added to 30 µl of washed and packed Dynabeads and 500 µl of RIPA Buffer and incubated at room temperature for 1 hour. Control beads were incubated with rabbit IgG. Beads were washed three times with RIPA buffer (500 µl). The bead–antibody complex was resuspended in 500 µl of RIPA Buffer with PI cocktail and 15 µg of the cell extract was added and samples incubated for 1 hour at room temperature with rotation. After several washes with 1 ml RIPA Buffer with PI cocktail, 30 µl of 1× Laemmli sample buffer with 20 mM DTT was added to the samples. Samples were heated at 100°C for 5 minutes and resolved on gels, transferred for immunoblotting, and processed as described above.

Statistics

We used either the Student's *t*-test (GraphPad Instat) or the Graphpad QuickCalc Chi-Square calculator (http://www.graphpad.com/quickcalcs/chisquared2.cfm) where appropriate, as indicated.

This work was supported by NIH grants EY08512 to M.A.S. and EY005665 to J.D.Z. Zeiss 710 confocal microscopy was made possible by NIH SIG grant F10 RR025565. We would also like to thank Ilene Gipson for the gift of the HCLE cell line; Anastas Popratiloff, director of the GWU Center for Microscopy and Image Analysis for help with imaging; Teresa Hawley, director of the FACs Core Facility at GWU, for help with flow cytometry. Deposited in PMC for release after 12 months.

Supplementary material available online at
http://jcs.biologists.org/cgi/content/full/124/15/2666/DC1

References

Borradori, L. and Sonnenberg, A. (1996). Hemidesmosomes: roles in adhesion, signaling and human diseases. *Curr. Opin. Cell Biol.* **8**, 647-656.

Chen, P., Abacherli, L. E., Nadler, S. T., Wang, Y., Li, Q. and Parks, W. C. (2009). MMP7 shedding of syndecan-1 facilitates re-epithelialization by affecting α2β1 integrin activation. *PLoS ONE* **4**, e6565.

Chetty, C., Lakka, S. S., Bhoopathi, P. and Rao, J. S. (2010). MMP-2 alters VEGF expression via αvβ3 integrin-mediated PI3K/AKT signaling in A549 lung cancer cells. *Int. J. Cancer* **127**, 1081-1095.

Choi, W. S., Jeon, O. H. and Kim, D. S. (2010). CD40 ligand shedding is regulated by interaction between matrix metalloproteinase-2 and platelet integrin αIIbβ3. *J. Thromb. Haemost.* **8**, 1364-1371.

Chotikavanich, S., de Paiva, C. S., Li, de-Q., Chen, J. J., Bian, F., Farley, W. J. and Pflugfelder, S. C. (2009). Production and activity of matrix metalloproteinase-9 on the ocular surface increase in dysfunctional tear syndrome. *Invest. Ophthalmol. Vis. Sci.* **50**, 3203-3209.

de Pereda, J. M., Ortega, E., Alonso-García, N., Gómez-Hernández, M. and Sonnenberg, A. (2009). Advances and perspectives of the architecture of hemidesmosomes: lessons from structural biology. *Cell Adh. Migr.* **3**, 361-364.

Dowling, J., Yu, Q. C. and Fuchs, E. (1996). β4 integrin is required for hemidesmosome formation, cell adhesion and cell survival. *J. Cell Biol.* **134**, 559-572.

Endo, K., Takino, T., Miyamori, H., Kinsen, H., Yoshizaki, T., Furukawa, M. and Sato, H. (2003). Cleavage of syndecan-1 by membrane type matrix metalloproteinase-1 stimulates cell migration. *J. Biol. Chem.* **278**, 40764-40770.

Gálvez, B. G., Matías-Román, S., Yáñez-Mó, M., Sánchez-Madrid, F. and Arroyo, A. G. (2002). ECM regulates MT1-MMP localization with β1 or αvβ3 integrins at distinct cell compartments modulating its internalization and activity on human endothelial cells. *J. Cell Biol.* **159**, 509-521.

Garrana, R. M., Zieske, J. D., Assouline, M. and Gipson, I. K. (1999). Matrix metalloproteinases in epithelia from human recurrent corneal erosion. *Invest. Ophthalmol. Vis. Sci.* **40**, 1266-1270.

Giancotti, F. G., Stepp, M. A., Suzuki, S., Engvall, E. and Ruoslahti, E. (1992). Proteolytic processing of endogenous and recombinant β4 integrin subunit. *J. Cell Biol.* **118**, 951-959.

Gipson, I. K. (1992). Adhesive mechanisms of the corneal epithelium. *Acta Ophthalmol. Suppl.* **202**, 13-17.

Gipson, I. K., Spurr-Michaud, S., Tisdale, A., Elwell, J. and Stepp, M. A. (1993). Redistribution of the hemidesmosome components α6β4 integrin and bullous pemphigoid antigens during epithelial wound healing. *Exp. Cell Res.* **207**, 86-98.

Gjelstrup, L. C., Boesen, T., Kragstrup,T. W., Jørgensen, A., Klein, N. J., Thiel, S., Deleuran, B. W. and Vorup-Jensen, T. (2010). Shedding of large functionally active CD11/CD18 Integrin complexes from leukocyte membranes during synovial inflammation distinguishes three types of arthritis through differential epitope exposure. *J. Immunol.* **185**, 4154-4168.

Hutcheon, A. E., Guo, X. Q., Stepp, M. A., Simon, K. J., Weinreb, P. H., Violette, S. M. and Zieske, J. D. (2005). Effect of wound type on Smad 2 and 4 translocation. *Invest. Ophthalmol. Vis. Sci.* **46**, 2362-2368.

Hutcheon, A. E., Sippel, K. C. and Zieske, J. D. (2007). Examination of the restoration of epithelial barrier function following superficial keratectomy. *Exp. Eye Res.* **84**, 32-38.

Kennel, S. J., Foote, L. J., Falcioni, R., Sonnenberg, A., Stringer, C. D., Crouse, C. and Hemler, M. E. (1989). Analysis of the tumor-associated antigen TSP-180. Identity with α6β4 in the integrin superfamily. *J. Biol. Chem.* **264**, 15515-15521.

Ludwig, A., Hundhausen, C., Lambert, M. H., Broadway, N., Andrews, R. C., Bickett, D. M., Leesnitzer, M. A. and Becherer, J. D. (2005). Metalloproteinase inhibitors for the disintegrin-like metalloproteinases ADAM10 and ADAM17 that differentially block constitutive and phorbol ester-inducible shedding of cell surface molecules. *Comb. Chem. High Throughput Screen.* **8**, 161-171.

Menon, B., Singh, M., Ross, R. S., Johnson, J. N. and Singh, K. (2006). β-Adrenergic receptor-stimulated apoptosis in adult cardiac myocytes involves MMP-2-mediated disruption of β1 integrin signaling and mitochondrial pathway. *Am. J. Physiol. Cell Physiol.* **290**, C254-C261.

Mohan, R., Chintala, S. K., Jung, J. C., Villar, W. V., McCabe, F., Russo, L. A., Lee, Y., McCarthy, B. E., Wollenberg, K. R., Jester, J. V. et al. (2002). Matrix metalloproteinase gelatinase B (MMP-9) coordinates and effects epithelial regeneration. *J. Biol. Chem.* **277**, 2065-2072.

Mol, M. A., van den Berg, R. M. and Benschop, H. P. (2009). Involvement of caspases and transmembrane metalloproteases in sulphur mustard-induced microvesication in adult human skin in organ culture: directions for therapy. *Toxicology* **258**, 39-46.

Morozevich, G., Kozlova, N., Cheglakov, I., Ushakova, N. and Berman, A. (2009). Integrin α5β1 controls invasion of human breast carcinoma cells by direct and indirect modulation of MMP-2 collagenase activity. *Cell Cycle* **8**, 2219-2225.

Nishizawa, Y., Uematsu, J. and Owaribe, K. (1993). HD4, a 180 kDa bullous pemphigoid antigen, is a major transmembrane glycoprotein of the hemidesmosome. *J. Biochem.* **113**, 493-501.

Onat, D. S., Jelic, S., Schmidt, A. M., Pile-Spellman, J., Homma, S., Padeletti, M., Jin, Z., LeJemtel, T. H., Colombo, P. C. and Feng, L. (2008). Vascular endothelial sampling and analysis of gene transcripts: a new quantitative approach to monitor vascular inflammation *J. Appl. Physiol.* **103**, 1873-1878.

Pajoohesh-Ganji, A., Ghosh, S. P. and Stepp, M. A. (2004). Regional distribution of α9β1 integrin within the limbus of the mouse ocular surface. *Dev. Dyn.* **230**, 518-528.

Pal-Ghosh, S., Pajoohesh-Ganji, A., Brown, M. and Stepp, M. A. (2004). A mouse model for the study of recurrent corneal epithelial erosions: α9β1 integrin implicated in progression of the disease. *Invest. Ophthalmol. Vis. Sci.* **45**, 1775-1788.

Pal-Ghosh, S., Tadvalkar, G., Jurjus, R. A., Zieske, J. D. and Stepp, M. A. (2008). BALB/c and C57BL6 mouse strains vary in their ability to heal corneal epithelial debridement wounds. *Exp. Eye Res.* **87**, 478-486.

Pflugfelder, S. C., Farley, W., Luo, L., Chen, L. Z., de Paiva, C. S., Olmos, L. C., Li, de-Q. and Fini, M. E. (2005). Matrix metalloproteinase-9 knockout confers resistance to corneal epithelial barrier disruption in experimental dry eye. *Am. J. Pathol.* **166**, 61-71.

Potts, A. J., Croall, D. E. and Hemler, M. E. (1994). Proteolytic cleavage of the integrin β4 subunit. *Exp. Cell Res.* **212**, 2-9.

Pruessmeyer, J., Martin, C., Hess, F. M., Schwarz, N., Schmidt, S., Kogel, T., Hoettecke, N., Schmidt, B., Sechi, A., Uhlig, S. et al. (2010). A disintegrin and metalloproteinase 17 (ADAM17) mediates inflammation-induced shedding of syndecan-1 and -4 by lung epithelial cells. *J. Biol. Chem.* **285**, 555-564.

Radjabi, A. R., Sawada, K., Jagadeeswaran, S., Eichbichler, A., Kenny, H. A., Montag, A., Bruno, K. and Lengyel, E. (2008). Thrombin induces tumor invasion through the induction and association of matrix metalloproteinase-9 and β1-integrin on the cell surface. *J. Biol. Chem.* **283**, 2822-2834.

Ramamurthi, S., Rahman, M. Q., Dutton, G. N. and Ramaesh, K. (2006). Pathogenesis, clinical features and management of recurrent corneal erosions. *Eye* **20**, 635-644.

Redondo-Muñoz, J., Ugarte-Berzal, E., García-Marco, J. A., del Cerro, M. H., Van den Steen, P. E., Opdenakker, G., Terol, M. J. and García-Pardo, A. (2008). α4β1 integrin and 190-kDa CD44v constitute a cell surface docking complex for gelatinase B/MMP-9 in chronic leukemic but not in normal B cells. *Blood* **112**, 169-178.

Schumann, H., Baetge, J., Tasanen, K., Wojnarowska, F., Schäcke, H., Zillikens, D. and Bruckner-Tuderman, L. (2000). The shed ectodomain of collagen XVII/BP180 is targeted by autoantibodies in different blistering skin diseases. *Am. J. Pathol.* **156**, 685-695.

Sta Iglesia, D. D. and Stepp, M. A. (2000). Disruption of the basement membrane after corneal débridement. *Invest. Ophthalmol. Vis. Sci.* **41**, 1045-1053.

Sta Iglesia, D. D., Gala, P. H., Qiu, T. and Stepp, M. A. (2000). Integrin expression during epithelial migration and restratification in the tenascin-C-deficient mouse cornea. *J. Histochem. Cytochem.* **48**, 363-376.

Stefanidakis, M., Ruohtula, T., Borregaard, N., Gahmberg, C. G. and Koivunen, E. (2004). Intracellular and cell surface localization of a complex between αMβ2 integrin and promatrix metalloproteinase-9 progelatinase in neutrophils. *J. Immunol.* **172**, 7060-7068.

Stepp, M. A., Spurr-Michaud, S., Tisdale, A., Elwell, J. and Gipson, I. K. (1990). α6β4 integrin heterodimer is a component of hemidesmosomes. *Proc. Natl. Acad. Sci. USA* **87**, 8970-8974.

Stepp, M. A., Liu, Y., Pal-Ghosh, S., Jurjus, R. A., Tadvalkar, G., Sekaran, A., Losicco, K., Jiang, L., Larsen, M., Li, L. et al. (2007). Reduced migration, altered matrix and enhanced TGFβ1 signaling are signatures of mouse keratinocytes lacking Sdc1. *J. Cell Sci.* **120**, 2851-2863.

Stepp, M. A., Pal-Ghosh, S., Tadvalkar, G., Rajjoub, L., Jurjus, R. A., Gerdes, M., Ryscavage, A., Cataisson, C., Shukla, A. and Yuspa, S. H. (2010). Loss of syndecan-1 is associated with malignant conversion in skin carcinogenesis. *Mol. Carcinog.* **49**, 363-373.

Suzuki, K., Tanaka, T., Enoki, M. and Nishida, T. (2000). Coordinated reassembly of the basement membrane and junctional proteins during corneal epithelial wound healing. *Invest. Ophthalmol. Vis. Sci.* **41**, 2495-2500.

Suzuki, K., Saito, J., Yanai, R., Yamada, N., Chikama, T., Seki, K. and Nishida, T. (2003). Cell-matrix and cell-cell interactions during corneal epithelial wound healing. *Prog. Retin. Eye Res.* **22**, 113-133.

Uitto, J. and Richard, G. (2004). Progress in epidermolysis bullosa: genetic classification and clinical implications. *Am. J. Med. Genet. C Semin. Med. Genet.* **131C**, 61-74.

Vaisar, T., Kassim, S. Y., Gomez, I. G., Green, P. S., Hargarten, S., Gough, P. J., Parks, W. C., Wilson, C. L., Raines, E. W. and Heinecke, J. W. (2009). MMP-9 sheds the β2 integrin subunit (CD18) from macrophages. *Mol. Cell. Proteomics* **8**, 1044-1060.

van der Neut, R., Krimpenfort, P., Calafat, J., Niessen, C. M. and Sonnenberg, A. (1996). Epithelial detachment due to absence of hemidesmosomes in integrin β4 null mice. *Nat. Genet.* **13**, 366-369.

von Bredow, D. C., Nagle, R. B., Bowden, G. T. and Cress, A. E. (1997). Cleavage of β4 integrin by matrilysin. *Exp. Cell Res.* **236**, 341-345.

Werner, M. E., Chen, F., Moyano, J. V., Yehiely, F., Jones, J. C. and Cryns, V. L. (2007). Caspase proteolysis of the integrin β4 subunit disrupts hemidesmosome assembly, promotes apoptosis, and inhibits cell migration. *J. Biol. Chem.* **282**, 5560-5569.

Zillikens, D. and Giudice, G. J. (1999). BP180/type XVII collagen: its role in acquired and inherited disorders or the dermal-epidermal junction. *Arch. Dermatol. Res.* **291**, 187-194.